

# Periodic-orbit resonance in the quasi-1D organic superconductor $(\text{TMTSF})_2\text{ClO}_4$

S. Takahashi,<sup>1</sup> S. Hill,<sup>1,\*</sup> S. Takasaki,<sup>2</sup> J. Yamada,<sup>2</sup> and H. Anzai<sup>2</sup>

<sup>1</sup>*Department of Physics, University of Florida, Gainesville, FL 32611, USA*

<sup>2</sup>*Department of Material Science, Graduate School of Science,*

*Himeji Institute of Technology, 3-2-1 Kouto, Kamigori-cho, Ako-gun, Hyogo 678-1297, Japan*

(Dated: September 28, 2018)

We report the observation of periodic-orbit resonance (POR) in a metal possessing pure quasi-one-dimensional (Q1D) Fermiology—namely, the organic linear-chain compound  $(\text{TMTSF})_2\text{ClO}_4$ , whose Fermi surface consists of a pair of weakly warped sheets. The POR phenomenon is related to weak inter-chain coupling, which allows electrons constrained on open trajectories to acquire small transverse velocities. Application of an appropriately oriented magnetic field induces periodic motion transverse to the chain direction and, hence, to a resonance in the AC conductivity. This resonance phenomenon is closely related to cyclotron resonance observed in metals with closed Fermi surfaces. For the Q1D POR, the field orientation dependence of the resonance is related simply to the Fermi velocity and lattice periodicity.

PACS numbers: 71.18.+y 72.15.Gd 74.70.Kn 76.40.+b

The organic metal  $(\text{TMTSF})_2\text{ClO}_4$  belongs to the family of quasi-one-dimensional (Q1D) Bechgaard salts<sup>1,2</sup> having the common formula  $(\text{TMTSF})_2\text{X}$ ; TMTSF is an abbreviation for tetramethyl-tetraselenafulvalene, and the anion X is  $\text{ClO}_4$ ,  $\text{PF}_6$ ,  $\text{ReO}_4$ , etc. For a long time,  $(\text{TMTSF})_2\text{X}$  was considered to be a conventional superconductor with a low  $T_c$  ( $\sim 1$  K). However, in the last few years, there have appeared clear evidences indicating an unconventional (triplet) character to the superconductivity in both the  $\text{X} = \text{ClO}_4$  and  $\text{PF}_6$  salts.<sup>3,4,5</sup> For example, Lee et al. have shown that the upper critical field ( $H_{c2}$ ) diverges as  $T \rightarrow 0$  for fields applied along certain directions.<sup>3,4</sup> This divergence is most pronounced in the  $\text{PF}_6$  salt (under pressure), with  $H_{c2}$  exceeding the Pauli paramagnetic limit by up to a factor of four.<sup>4</sup> Furthermore, <sup>77</sup>Se NMR studies reveal no Knight shift upon cooling through the superconducting transition, again suggesting spin-triplet pairing.<sup>5</sup>

Recent theoretical studies<sup>6,7,8</sup> have shown that the superconductivity in Q1D systems may depend strongly on the nesting properties of the Fermi surface (FS), as well as on the conduction bandwidth. Therefore, it is important to be able to make detailed measurements of their band structures and FS topologies. The FS of  $(\text{TMTSF})_2\text{ClO}_4$  reflects its crystal structure, which has a highly anisotropic character.<sup>2</sup> The planar TMTSF cations stack face-to-face in columns along the crystallographic  $a$ -axis. These columns then form layers parallel to the  $ab$ -plane. The strongest overlap between the partially occupied  $\pi$ -orbitals on the TMTSF molecules occurs along the columns. Therefore, the conductivity is highest (bandwidth is greatest) along the  $a$ -axis. The orbital overlap between the TMTSF columns, *i.e.* within the layers (intermediate direction), is about 10 times less, while the bandwidth is considerably weaker in the interlayer direction.<sup>9,10</sup> The electronic band structure may be calculated using a tight binding approximation. The anisotropy of the tight binding transfer integrals ( $t_a : t_b : t_c$ ) is about 200:20:1 meV. As a result, the

FS consists of a pair of weakly warped sheets,<sup>10</sup> oriented perpendicular to the  $a$ -axis (see Fig. 1), *i.e.* the FS may be regarded as Q1D.

DC magnetoresistance measurements have proven to be very useful in determining the FS topologies of low-dimensional organic conductors.<sup>2,11,12,13,14,15,16,17</sup> In particular, a number of interesting effects are observed when measurements are made as a function of magnetic field orientation – so-called Angle-dependent Magneto-Resistance Oscillations (AMRO). As we have demonstrated in recent studies of numerous quasi-two-dimensional (Q2D) organic conductors, additional important information may be obtained from high frequency (microwave) AMRO studies.<sup>18,19,20</sup> High frequency implies  $\omega\tau > 1$  ( $\tau^{-1} \equiv$  scattering rate), and that  $2\pi/\omega$  is comparable to the period of any electronic motion caused by the application of a magnetic field (see below). Here, we report similar measurements for the pure Q1D  $(\text{TMTSF})_2\text{ClO}_4$  system. Semiclassical calculations show that a special kind of Q1D cyclotron resonance (CR), or periodic-orbit resonance (POR<sup>18</sup>), should be observed.<sup>18,19,20,21,22</sup> Indeed, this behavior is closely related to the semiclassical Q1D AMRO first discussed by Osada.<sup>11</sup> Using this effect, one can determine the Fermi velocity ( $v_F$ ) for  $(\text{TMTSF})_2\text{ClO}_4$  without dependence on any parameters other than the lattice periodicity. The idea of cyclotron orbits in a Q1D system should not be taken literally. Nevertheless, *it is* the Lorentz force which causes the periodic electronic motion which ultimately gives rise to this unusual POR phenomenon, as we now briefly describe with the aid of Fig. 1. We note that our discussion of the POR is based on the semiclassical Boltzmann transport equation.<sup>11</sup> We discuss the validity of this approach later in this article.

Due to the finite bandwidth (finite orbital overlap) in the intermediate conductivity direction, the FS sheets become warped, as represented by the corrugations in Fig. 1. This warping may be decomposed into Fourier harmonics, each characterized by some vector  $\mathbf{R}$  in real

space. In fact, one expects a different warping vector for every finite transfer integral. Thus, in general, one requires a set of indices  $(m, n)$  in order to keep track of all of the warping harmonics  $\mathbf{R}_{m,n}$ . However, due to the simplicity of the experimental data, we restrict the following discussion to a single vector  $\mathbf{R}_{\parallel}$  (Fig. 1), representing the projection of a single warping vector onto the plane of the FS. In the presence of a magnetic field ( $B$ ), an electron moves along the FS with a constant rate of change of momentum ( $\hbar dk/dt$ ) in a plane perpendicular to the magnetic field, and with its velocity always directed perpendicular to the FS. Thus, its motion is mainly directed along the  $a$ -axis ( $v_{\parallel}$ ). However, due to the periodic FS corrugations, the electron's transverse velocity ( $v_{\perp}$ ) oscillates slightly about zero (see trajectory in Fig. 1). In general, for a three dimensional FS, this effect gives rise to periodic oscillations of both velocity components within the plane of the Q1D FS ( $b'c^*$ -plane in this case). The frequency of these oscillations is proportional to (i) the magnitude of  $\mathbf{R}_{\parallel}$ , and (ii) the magnetic field component perpendicular to the warping vector ( $\mathbf{R}_{\parallel}$ ) and parallel to the FS. Each harmonic of the warping, therefore, gives rise to a distinct resonance in the  $b'c^*$ -plane microwave conductivity, with a frequency that scales with  $B$ , as is also the case for conventional CR. Meanwhile, each Q1D resonance has a distinct angle dependence characterized by the warping vector  $\mathbf{R}_{\parallel}$ . However, instead of the CR mass, the resonance frequency  $\nu$  depends on the Q1D Fermi velocity ( $v_F$ ) though the following equations:<sup>19,21</sup>

$$\frac{\nu}{B_{res}} = \frac{ev_F R_{\parallel}}{\hbar} |\sin(\theta_{b'c^*} - \theta_o)|, \quad (1a)$$

$$\frac{\nu}{B_{res}} = \frac{ev_F R_{\parallel}}{\hbar} |\cos(\theta_{\perp}) \sin(\theta'_o)|. \quad (1b)$$

Eq. 1(a) corresponds to magnetic field rotations parallel to the plane of the FS;  $\theta_{b'c^*}$  is the angle between  $c^*$  and the projection of  $B$  onto the  $b'c^*$ -plane; and  $\theta_o$  represents the angle between  $c^*$  and  $\mathbf{R}_{\parallel}$ . Eq. 1(b) corresponds to magnetic field rotations away from the  $b'c^*$ -plane, towards the  $a$ -axis (i.e. in a plane  $\perp$  to the FS);  $\theta_{\perp}$  is the angle between the  $b'c^*$ -plane and  $B$ ; and  $\theta'_o$  represents the angle between the plane of rotation and  $\mathbf{R}_{\parallel}$ . Finally, in both cases,  $B_{res}$  is the resonance field. These geometries are depicted in Fig. 1. It is the conductivity parallel to the Q1D Fermi surface ( $b'c^*$ -plane) which has a maximum at the resonance, and the amplitude of the resonance is proportional to the amplitude of the relevant Fourier component ( $G_{m,n}$ ) of the FS corrugation. Thus, angle dependent measurements enable a determination of the orientations of warping vectors (or transfer integrals). A more general expression for a material possessing a Q1D FS with many warping components is given in ref. [19]. While similar information may also be deduced from DC AMRO ( $\nu \sim 0$ ), one obtains only the directions of warping vectors from such studies, i.e. AMRO

are observed at the zeros of Eq. 1(a), where  $\theta_{b'c^*} = \theta_o$ . On the other hand, finite frequency Q1D POR additionally enables a determination of the product  $v_F R_{\parallel}$  (see Eq. 1). Since the warping vectors ( $\mathbf{R}_{m,n}$ ) are usually related to the underlying lattice constants, which are well known from X-ray data, Q1D POR provides the most direct means of measuring  $v_F$  in Q1D metals. Until now, this technique has been limited to systems with strongly warped open FS sections (i.e. Q2D systems), leading to a strong harmonic content of the POR.<sup>19,22,23</sup> The present study is the first of its kind for a member of the widely studied Q1D (TMTSF)<sub>2</sub>X family. We note that a previous investigation within the field-induced-spin-density-wave (FISDW) phase of (TMTSF)<sub>2</sub>ClO<sub>4</sub> ( $B > 6$  T,  $T \sim 1.2$  K) tentatively ascribed several dips in the far-infrared magneto-reflectivity to inter-Landau-level (i.e. CR-like) transitions across the FISDW gap.<sup>24</sup>

Microwave measurements were carried out using a millimeter-wave vector network analyzer and a high sensitivity cavity perturbation technique; this instrumentation is described in detail elsewhere.<sup>25</sup> In order to enable in-situ rotation of the sample relative to the applied magnetic field, we employed two methods. The first involved a split-pair magnet with a 7 T horizontal field and a vertical access. Smooth rotation of the entire rigid microwave probe, relative to the fixed field, was achieved via a room temperature stepper motor (with 0.1° resolution). The second method involved in-situ rotation of the end-plate of a cylindrical cavity, mounted with its axis transverse to a 17 T superconducting solenoid. Details concerning this cavity, which provides an angle resolution of 0.18°, have been published elsewhere.<sup>26</sup> Several needle shaped samples were separately investigated by placing them in one of two geometries within the cylindrical TE011 cavities, enabling (i) field rotation in the  $b'c^*$ -plane, and (ii) rotation away from the  $b'c^*$ -plane towards the  $a$ -axis. Each sample was slowly cooled ( $< 0.1$  K/min between 32 K and 17 K) through the anion ordering transition at 24 K to obtain the low-temperature metallic state.<sup>2</sup> All experiments were performed at 2.5 K, and data for two of the samples are presented in this paper (labeled A and B, dimensions  $\sim 1 \times 0.2 \times 0.1$  mm<sup>3</sup>). In order to verify that the relaxed state is reproducibly achieved, we can observe signatures of the FISDW phase transition in the microwave response (see Fig. 2) for experiments conducted in the 17 T magnet. Studies of the angle dependence of the FISDW transition also allow us to determine the orientations of the  $b'$  and  $c^*$  directions in-situ, i.e. simultaneous to the POR measurements.

In Fig. 2, we present 61.8 GHz absorption data for sample A (2nd cooling) in fields up to 15 T. The magnetic field was rotated in the  $b'c^*$ -plane ( $\perp$  needle axis), and successive traces were taken in 8.8° steps; the angle ( $\theta_{b'c^*}$ ) refers to the field orientation relative to the  $c^*$  axis. Two pronounced angle-dependent features are apparent in the data. At the lowest fields, a peak in absorption is observed (labeled POR) which moves to higher magnetic fields upon rotating the field away from the  $b'$  direction

( $\theta_{b'c^*} = 90^\circ$ ). It is this peak which corresponds to the POR. Its position in field is proportional to the frequency (not shown), as expected for a cyclotron-like resonance. At higher fields (above  $\sim 9$  T), a sharp kink in the absorption is observed (labeled  $B_{\text{FISDW}}$ ), which moves to higher fields upon rotating the field away from the  $c^*$  direction ( $\theta_{b'c^*} = 0^\circ$ ). The position of this feature does not depend on the measurement frequency. In fact, its angle and temperature dependence are in excellent agreement with the expected behavior of the  $N = 0$  FISDW phase boundary.<sup>2,27</sup> We are thus able to use the angle-dependence of this kink to determine the field orientation relative to the  $b'$  and  $c^*$  directions. Qualitatively similar POR data were obtained for this (1st cooling) and other samples in the lower field magnet, both for  $b'c^*$ -plane field rotations and for rotations away from the  $b'c^*$ -plane (see Fig. 3).

For all measurements reported in this paper, the sample was positioned within the cavity in such a manner so as to excite currents in the low conductivity  $b'c^*$ -plane, as required for Q1D POR. In fact, it is very difficult to measure the  $a$ -axis conductivity using the cavity perturbation technique. The penetration depths for the typical frequencies used in this study are of order  $100 \mu\text{m}$  for currents along  $c^*$ , and  $5 \mu\text{m}$  for currents along  $b'$ . Consequently, the electromagnetic fields penetrate well into the sample, thus accounting for the approximately Lorentzian CR lineshape which is characteristic of the bulk conductivity.<sup>28</sup> This rules out any possibility that the observed resonance could be due to the Azbel'-Kaner-type CR originally predicted for Q1D conductors by Gor'kov and Lebed.<sup>29</sup> In particular, one would expect to observe several CR harmonics in such a case, but only for the surface resistance parallel to  $a$ . Furthermore, it is unlikely that the conditions for the Gor'kov and Lebed CR could ever be satisfied in  $(\text{TMTSF})_2\text{ClO}_4$ , namely that the  $b'$ -axis penetration depth ( $\sim 3 - 5 \mu\text{m}$ ) be considerably less than the amplitude of the  $b'$ -axis motion ( $\sim 0.1 \mu\text{m}$  at 2 tesla) caused by the FS corrugations (see Fig. 1) and, simultaneously,  $\omega_c\tau \gg 1$ .

In Fig. 3a we plot the  $b'c^*$ -plane angle dependence of the ratio  $\nu/B_{\text{res}}$  for two samples (A and B), and for several measurement frequencies.  $B_{\text{res}}$  is determined simply from the position of maximum absorption due to the POR (low field dashed curve in Fig. 2). The POR data (open symbols) agree extremely well with Eq. 1a (solid curves), with relatively little scatter in the data for the various measurements. Also displayed in Fig. 3a is the angle-dependence of the FISDW transition field,  $B_{\text{FISDW}}$  (solid squares). These data scale with the inverse of the cosine of the angle  $\theta_{b'c^*}$  (dashed curve), reflecting the 2D nature of the standard theory of the FISDW.<sup>2,27</sup> From the  $1/\cos\theta_{b'c^*}$  fits to  $B_{\text{FISDW}}$ , we see that the zeros in  $B_{\text{res}}$  (equivalent to  $m/n = p/q = 0$  AMRO minima) occur when the field is parallel to the  $c'$  direction ( $\sim 5^\circ$  away from  $c^*$ ), in excellent agreement with DC AMRO measurements.<sup>14,15,17,30,31</sup> In Fig. 3b we plot the ratio  $\nu/B_{\text{res}}$  for sample A, for rotation away from the  $b'c^*$

plane. In this case, the zeros in  $\nu/B_{\text{res}}$  were found to lie exactly along the  $a$ -axis of the crystal, as expected from Eq. 1b. The reason for the discrepancy between the maximum value of  $\nu/B_{\text{res}}$  in Figs. 3a and 3b is due to the fact that the orientation of the  $c^*$ -axis was not well known when mounting the sample for the rotations away from the  $b'c^*$  plane, resulting in a mis-alignment between the plane of rotation and  $c^*$ , i.e. a finite  $\theta'_0$  (Eq. 1b), thus diminishing the maximum in  $\nu/B_{\text{res}}$ .

It is important to stress that the POR phenomenon (semiclassical AMRO) is entirely expected if one assumes a 3D band structure along with the accepted 3D hopping matrix elements. This idea was first discussed for the case of the Bechgaard salts by Osada,<sup>11</sup> and has subsequently been adapted by many authors to account for both DC and high-frequency conductivity resonances observed in several Q2D BEDT-TTF salts.<sup>19,20,21,22,32</sup> However, one has to consider whether a 3D band transport picture is appropriate for the Bechgaard salts in view of their extreme low-dimensionality. Indeed, Lebed's original explanation for the so-called "magic-angle effects" (or "Lebed resonances") involves a magnetic-field-induced dimensional crossover. Application of a magnetic field perpendicular to the least conducting  $c^*$  direction has the effect of localizing/confining quasiparticles to a single layer, resulting in a crossover from coherent (3D band transport) to incoherent interlayer transport at relatively weak fields. The three dimensionality is subsequently restored whenever the applied field direction is commensurate with any intermolecular hopping direction,  $\mathbf{R}_{m,n}$ .<sup>33,34</sup> These changes in effective dimensionality are expected to have a profound effect on electronic correlations, ultimately giving rise to the Lebed resistance resonances. However, Lebed's magic-angles are indistinguishable from the DC AMRO directions in Osada's theory.<sup>11,32</sup> Consequently, a consensus has not yet emerged concerning the explanation for the Lebed resonances seen in  $(\text{TMTSF})_2\text{X}$ .

Lebed's theory differs from Osada's in the sense that the "magic-angles" really are magic, i.e. the underlying dimensionality of the electronic system changes from two- to three- at these angles. Consequently, one *should not* observe Lebed resonances in an experiment such as the one reported here, where the field orientation is fixed. In contrast, there are no "magic-angles" in Osada's theory. Conductivity resonances occur at frequencies and angles given by  $\omega = v_F G_{m,n}$ , where the  $G_{m,n}$  characterize the Fourier components of the FS warping.<sup>11</sup> The zeros of  $G_{m,n}$  determine the DC ( $\omega = 0$ ) AMRO minima. However, for  $\omega \approx v_F R_{\parallel} eB/\hbar$ , the AMRO directions are determined instead by the zeros of  $(\omega - v_F G_{m,n})$ , i.e. they shift with field and frequency. Consequently, one *does* observe these resonances by fixing the field orientation and sweeping only its magnitude. Indeed, the fit to the resonance positions in Fig. 3 corresponds precisely to the zeros of  $(\omega - v_F G_{01})$ , and the data intersect the  $\nu = 0$  axis at precisely the expected angles corresponding to the  $p/q = 0$  ( $\equiv m/n$ ) Lebed resonances.

Based on the above discussion, and Fig. 3, our findings appear to support Osada’s theory. However, a surprising aspect of the data is the lack of any significant harmonic content to the POR. In contrast, low-temperature DC AMRO studies reveal several dips in both the interlayer ( $\parallel c^*$ ) and in-plane ( $\parallel a$ ) resistivities, corresponding to different ratios of the indices  $p$  and  $q$  which are commonly used to index AMRO harmonics.<sup>14,15,17,30,31</sup> Strong harmonics are also clearly seen, even in the POR data, for the organic conductor  $\alpha$ -(ET)<sub>2</sub>KHg(SCN)<sub>4</sub>,<sup>19</sup> although this material has a Q2D band structure, its low-temperature electronic properties are dominated by a strongly corrugated Q1D (open) FS which results from the reconstruction of a high-temperature ( $> 8$  K) Q2D FS.<sup>32</sup> The high harmonic content of the POR observed in  $\alpha$ -(ET)<sub>2</sub>KHg(SCN)<sub>4</sub> is a direct of this unusual low-temperature FS.<sup>32</sup> In contrast, (TMTSF)<sub>2</sub>ClO<sub>4</sub> really is a Q1D conductor, i.e. one can practically neglect higher order hopping terms (next-nearest-neighbor, etc..) in a tight-binding description of the  $b'c'$ -plane band dispersion. Consequently, the FS warping will be dominated by the  $G_{01}$  and  $G_{10}$  Fourier harmonics, and it is reasonable to expect higher-order POR harmonics to be significantly weaker than the fundamental  $p/q = 0$  resonance. Nevertheless, significant higher-order content has convincingly been reported in DC AMRO experiments with ratios of  $p/q$  up to 5.<sup>31</sup> It should be noted, however, that all DC AMRO experiments reporting high-harmonic content were performed either on the X = PF<sub>6</sub> salt (under pressure), and/or at considerably lower temperatures ( $< 1$  K) and higher fields than the present investigation.<sup>14,15,17,30,31</sup> In fact, there is a very limited amount of published DC AMRO data for (TMTSF)<sub>2</sub>ClO<sub>4</sub>, obtained at comparable fields and temperatures to the present investigation ( $T = 2.5$  K and  $B \sin \theta < 3$  T), and those that can be found reveal no evidence for higher order harmonics, i.e. only the  $p/q = 0$  resonance is seen. Comparisons are also complicated by the fact that our experiments are performed at fixed field orientations, whereas DC AMRO are necessarily observed by rotating the magnetic field direction. Furthermore, for most of the angles in the present investigation, the  $p/q > 0$  harmonics would be expected at fields well below the  $p/q = 0$  fundamental resonance. Therefore, on the basis of comparisons with published DC AMRO data, it is *not* surprising that the  $p/q > 0$  harmonics are not observed within the parameter space available for these experiments. Future instrument developments will be aimed at enabling angle-dependent measurements at lower temperatures, as well as studying the X = PF<sub>6</sub> salt under pressure.

Due to the mechanics of our experiment, we can make no statements about “magic-angle-effects”. Indeed, it is quite possible that the Lebed resonances are missed entirely in this investigation. However, we wish to emphasize that the observed POR are precisely the same phenomenon as the semiclassical AMRO discussed by Osada,<sup>11</sup> and by many other authors in subsequent

papers.<sup>19,20,21,22,32</sup> We now know from these investigations that the  $p/q = 0$  POR resonance is not “magic” in the sense that its orientation varies with frequency (Fig. 3). Whether or not the Lebed resonances are observable at microwave frequencies, and whether this really is a “magic-angle effect” remains to be seen. One intriguing possibility that cannot be ruled out is that there is an interplay between both effects, and that the magic-angle physics dominates the DC AMRO at high fields and low temperatures, causing strong AMRO harmonics, whereas the present microwave studies are sensitive only to the semiclassical physics.

From an analysis of the POR line shape (Fig. 2), we estimate a relaxation time of about 4 ps. This is close to the typical value estimated from the field dependence of the DC magnetoresistance (1–5 ps) of a relaxed sample.<sup>13</sup> Based on this, and on the known interlayer bandwidth, we can conclude that (TMTSF)<sub>2</sub>ClO<sub>4</sub> exhibits truly coherent 3D band transport at low fields. However, application of a field within the layers will obviously change this picture. Nevertheless, we believe that this lends further support to our assertion that the POR observed in this study correspond to the high-frequency AMRO first discussed by Osada,<sup>11</sup> and there is no need to consider alternative models such as those developed for incoherent interlayer transport.<sup>35</sup>

We next turn to the pre-factor  $A_o$  ( $\equiv ev_F R_{\parallel}/h$ ) in Eq. 1. From these studies, we obtain a single value of 24(1) GHz/T. However, earlier studies on older samples (not shown) gave values in the 30 – 34 GHz/tesla range. These differences are not fully understood. However, a possible explanation is the rather small  $\omega\tau$  product ( $\sim 2$ ), and instrumental factors which give rise to distorted CR lineshapes for some samples. We note that the  $\nu/B_{res}$  maximum is determined by the lowest-field resonances. Therefore, although we correct distorted lineshapes (an advantage to measuring phase shift in addition to absorption<sup>25</sup>), a small systematic error may easily account for a 10 – 15% shift in  $A_o$ . Still, this is not enough to account for the differences between this and earlier studies. In fact, samples with the smallest  $A_o$  values give appreciably broader resonances (increase in  $\tau$  of 30%) relative to the samples A and B used in this study, suggesting that samples used in earlier studies may not have attained the fully ordered metallic state. This raises the intriguing possibility that perhaps  $A_o$  and, therefore  $\nu_F$ , depends on cooling rate, i.e. the closer proximity to the insulating state results in a reduction in  $\nu_F$ , or larger effective mass.

Finally, we turn to the value of  $\nu_F$ . Since the zeros in  $\nu/B_{res}$  occur when the field is along  $c'$ , the appropriate value for  $R_{\parallel}$  is 13.2 Å.<sup>2</sup> This gives rise to a Fermi velocity of  $0.76(3) \times 10^5$  m/s. This is within a factor of two of the value estimated from specific heat measurements ( $1.4 \times 10^5$  m/s),<sup>36</sup> and in close agreement with the value estimated from recent transport measurements ( $3 - 6 \times 10^4$  m/s).<sup>16</sup>

In conclusion, we have observed periodic-orbit reso-

nances for the first time in a purely Q1D organic conductor. The behavior is dominated by the  $c'$ -axis dispersion. This technique provides one of the most direct methods for determining key band structure parameters which may be important for understanding the unconventional superconductivity in the  $(\text{TMTSF})_2\text{X}$  family.

We are grateful to A. E. Kovalev and J.S. Brooks for their contributions to these studies. This work was supported by the National Science Foundation (DMR0196461 and DMR0239481). S. H. acknowledges the Research Corporation for financial support.

- 
- \* corresponding author, Email:hill@phys.ufl.edu
- <sup>1</sup> K. Bechgaard, C. S. Jacobsen, K. Mortensen, H. J. Pedersen, and N. Thorup, *Solid State Commun.* **33**, 1119 (1980).
  - <sup>2</sup> T. Ishiguro, K. Yamaji, and G. Saito, *Organic Superconductors*, vol. 88 of *Springer Series in Solid State Sciences* (Springer-Verlag, Berlin, 1998).
  - <sup>3</sup> I. J. Lee, A. P. Hope, M. J. Leone, and M. J. Naughton, *Synth. Met.* **70**, 747 (1995).
  - <sup>4</sup> I. J. Lee, P. M. Chaikin, and M. J. Naughton, *Phys. Rev. B* **62**, R14669 (2000).
  - <sup>5</sup> I. J. Lee, S. E. Brown, W. G. Clark, M. J. Strouse, M. J. Naughton, W. Kang, and P. M. Chaikin, *Phys. Rev. Lett.* **88**, 017004 (2002).
  - <sup>6</sup> R. Louati, S. Charfi-Kaddour, A. BenAli, R. Bennaceur, and M. Héritier, *Phys. Rev. B* **62**, 5957 (2000).
  - <sup>7</sup> Y. Tanuma, K. Kuroki, Y. Tanaka, R. Arita, S. Kashiwaya, and H. Aoki, *Phys. Rev. B* **66**, 094507 (2002).
  - <sup>8</sup> R. W. Cherng and C. A. R. SadeMelo, *Phys. Rev. B* **67**, 212505 (2003).
  - <sup>9</sup> K. Kikuchi, I. Ikemoto, K. Yakushi, H. Kuroda, and K. Kobayashi, *Solid State Commun.* **42**, 433 (1982).
  - <sup>10</sup> P. M. Grant, *Journale de Physique Colloque* **44**, 847 (1983).
  - <sup>11</sup> T. Osada, S. Kagoshima, and N. Miura, *Phys. Rev. B* **46**, 1812 (1992).
  - <sup>12</sup> G. M. Danner, W. Kang, and P. M. Chaikin, *Phys. Rev. Lett.* **72**, 3714 (1994).
  - <sup>13</sup> E. I. Chashechkina and P. M. Chaikin, *Phys. Rev. B* **56**, 13658 (1997).
  - <sup>14</sup> E. I. Chashechkina and P. M. Chaikin, *Phys. Rev. Lett.* **80**, 2181 (1998).
  - <sup>15</sup> I. J. Lee and M. J. Naughton, *Phys. Rev. B* **58**, R13343 (1998).
  - <sup>16</sup> K. Kobayashi, E. Ohmichi, and T. Osada, *J. Phys. Chem. Solids* **63**, 1267 (2002).
  - <sup>17</sup> W. Kang, H. Kang, Y. J. Jo, and S. Uji, *Synth. Met.* **133-134**, 15 (2003).
  - <sup>18</sup> S. Hill, *Phys. Rev. B* **55**, 4931 (1997).
  - <sup>19</sup> A. E. Kovalev, S. Hill, and J. S. Qualls, *Phys. Rev. B* **66**, 134513 (2002).
  - <sup>20</sup> A. E. Kovalev, S. Hill, K. Kawano, M. Tamura, T. Naito, and H. Kobayashi, *Phys. Rev. Lett.* **91**, 216402 (2003).
  - <sup>21</sup> S. J. Blundell, A. Ardavan, and J. Singleton, *Phys. Rev. B* **55**, R6129 (1997).
  - <sup>22</sup> A. Ardavan, J. M. Schrama, S. J. Blundell, J. Singleton, W. Hayes, M. Kurmoo, P. Day, and P. Goy, *Phys. Rev. Lett.* **81**, 713 (1998).
  - <sup>23</sup> Y. Oshima, M. Kimata, K. Kishigi, H. Ohta, K. Koyama, M. Motokawa, H. Nishikawa, K. Kikuchi, and I. Ikemoto, *Phys. Rev. B* **68**, 054526 (2003).
  - <sup>24</sup> A. S. Perel, J. S. Brooks, C. J. G. N. Langerak, T. J. B. M. Janssen, J. Singleton, J. A. A. J. Perenboom, and L. Y. Chiang, *Phys. Rev. Lett.* **67**, 2072 (1991).
  - <sup>25</sup> M. Mola, S. Hill, P. Goy, and M. Gross, *Rev. Sci. Instrum.* **71**, 186 (2000).
  - <sup>26</sup> S. Takahashi and S. Hill, *Rev. Sci. Instr.* **76**, 023114 (2005).
  - <sup>27</sup> T. Osada, H. Nose, and M. Karaguchi, *Physica B* **294-295**, 402 (2001).
  - <sup>28</sup> S. Hill, *Phys. Rev. B* **62**, 8699 (2000).
  - <sup>29</sup> L. P. Gor'kov and A. G. Lebed', *Phys. Rev. Lett.* **71**, 3874 (1993).
  - <sup>30</sup> T. Osada, A. Kawasumi, S. Kagoshima, N. Miura, and G. Saito, *Phys. Rev. Lett.* **66**, 1525 (1991).
  - <sup>31</sup> M. J. Naughton, O. H. Chung, M. Chaparala, X. Bu, and P. Coppens, *Phys. Rev. Lett.* **67**, 3712 (1991).
  - <sup>32</sup> S. J. Blundell and J. Singleton, *Phys. Rev. B* **53**, 5609 (1996).
  - <sup>33</sup> A. G. Lebed, *Pis'ma Zh. Eksp. Teor. Fiz.* **43**, 137 (1986).
  - <sup>34</sup> A. G. Lebed and P. Bak, *Phys. Rev. Lett.* **63**, 1315 (1989).
  - <sup>35</sup> R. H. McKenzie and P. Moses, *Phys. Rev. B* **60**, R11241 (1999).
  - <sup>36</sup> P. Garoche, R. Brusetti, D. Jerome, and K. Bechgaard, *J. Phys. (France) Lett.* **43**, L147 (1982).

## Figure captions

FIG. 1: Schematic of a Q1D FS ( $\parallel b'c^*$ -plane) with arbitrary warping. The angles and vectors are described in the main text immediately after Eq. 1. Application of a magnetic field causes electrons to traverse the FS in a plane perpendicular to  $B$ . This reciprocal-space motion across the FS corrugations results in a periodic modulation of the real space velocity transverse to  $a$ , as represented by the wavy arrow.

FIG. 2: Angle dependent microwave absorption for sample A (2nd cooling) for rotations in the  $b'c^*$ -plane. Data were obtained between  $\theta_{b'c^*} = -62.7^\circ$  and  $7.6^\circ$  at  $8.8^\circ$  intervals; the frequency was 61.8 GHz and the temperature 2.5 K. The peaks in absorption are due to POR, and the kink at high fields is due to the FISDW transition. Both features are angle dependent.

FIG. 3: Angle dependence of the quantity  $\nu/B_{res}$  for (a)  $b'c^*$ -plane rotations (Eq. 1a), and (b) rotations away from the  $b'c^*$ -plane towards  $a$  (Eq. 1b); the inserts depict the experimental geometries. Data were obtained for two samples (A and B); A1 and A2 denote successive cool downs for sample A. The solid curves are fits to Eq. 1, and the directions of high symmetry are indicated in the figure. The experiments were all performed at 2.5 K, and at frequencies ranging from 45 to 69 GHz (not labeled). The quantity  $\nu/B_{res}$  is frequency independent to within the scatter of the data. In Fig. 1(a), the angle dependence of  $\nu/B_{FISDW}$  is also shown (filled squares), where  $\nu = 61.8$  GHz; these data have been fit to an inverse cosine function (dashed curve), enabling an accurate determination of the  $b'$  and  $c^*$  directions.

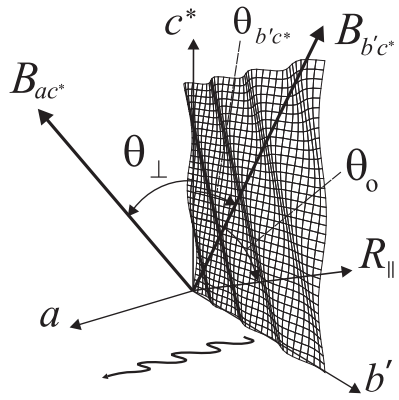


FIG. 1: S. Takahashi et al.

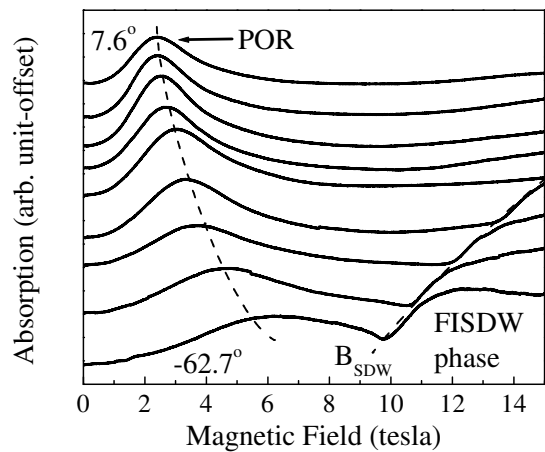


FIG. 2: S. Takahashi et al.

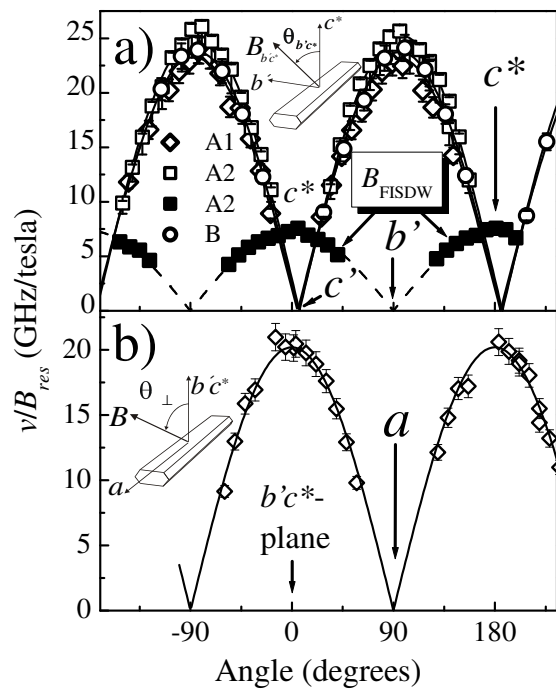


FIG. 3: S. Takahashi et al.